Output Enhancement of Bifacial Solar Modules Under Diffuse and Specular Albedo

Shweta Pal[1] and Rebecca Saive[1]

[1]University of Twente, Overijssel, Enschede, 7522NB, the Netherlands

***Abstract*— We present an albedo-centric reverse-ray tracing software to model the influence of albedo surfaces with complex spectro-angular reflectance (*i.e.* diffuse, glossy, specular, and metamaterials) on the short-circuit current density of a bifacial module. We find that for a silicon heterojunction module, a diffuse albedo leads to higher output and is more robust to self-shading and changes in orientation than a specular reflector. Our approach enables detailed and accurate albedo-dependent output calculation for various known and even exotic reflectors. Such a methodology can be used to design optimal reflectors and determine optimal configurations.**

Keywords—Reverse ray-tracing, Spectro-angular albedo, Diffuse albedo, Glossy albedo, Specular albedo, Short-circuit current density, Bifacial modules

I. Introduction

Bifacial modules, *i.e.*, modules that accept light from front and rear, offer a great opportunity for power output enhancements and cost reduction of solar generated electricity. A key component for bifacial module performance is the albedo, *i.e.*, ground-reflected irradiance. By improving the albedo, ground-sculpting [1, 2] configurations, for example, have promised significant output enhancement. Recent studies are recognizing the importance of quantifying spectral albedo for accurate output calculations [3, 4, 5]. Similarly, the spectral and angular dependence of incoming irradiance must be taken into account for accuracy—errors of up to 15% in output estimation for mono-crystalline silicon modules have been demonstrated without this quantification [6]. These become especially important for cells incorporating nanophotonic modifications [7] which promote light redirection [8] or trapping [9]. Various ray-tracing algorithms have been developed to understand the albedo-dependent PV output [10, 11, 12, 13]. Yet an extensive study on the effect of the spectro-angular albedo on bifacial modules is missing.

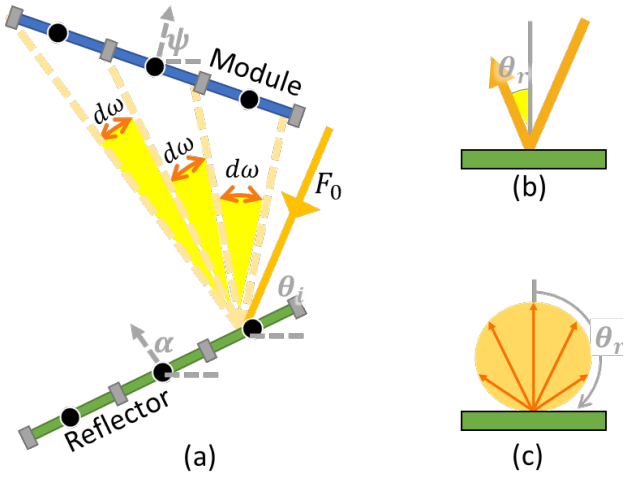

Fig. 1. Schematic of a) the definitions used in the code, b) mirror reflector, c) diffuse reflector.

To bridge this gap, we developed an in-house reverse ray-tracing software. The reverse ray-tracing is done from the perspective of the albedo, *i.e.*, the ground reflector. In this work, we performed the computation for a silicon heterojunction bifacial module (bifaciality = 98.8%) and calculated its short-circuit current density (J_{sc}). The calculated short-circuit current density will also be referred to as 'current density' or 'output' in the manuscript. The resulting software can generate various types of reflectors—diffuse, mirror and glossy—including the spectral and angular reflectivity. Custom spectral and angular reflectivity can also be implemented in the code. Such a methodology can facilitate in devising novel reflectors and their optimal configurations.

II. In-House Reverse Ray Tracing Software

Our goal is to determine the performance enhancement in bifacial modules with a bifaciality of 98.8% caused by various albedo surfaces, while taking both spectral and angular reflectivity into account. To properly account for complicated reflectivity while keeping the computation time reasonable, we employ reverse ray-tracing from the perspective of the reflector.

The code begins by defining a module (blue line in Fig. 1a and 1b) and a reflector (green line). We divide the total width of a surface into d pixels per unit length. Next, we implement reverse ray-tracing by illuminating each pixel on the reflector with one parallel ray of spectral flux, F_0, at the desired angle of incidence, θ_i, (solid yellow arrow).

The reflection function for a specular (f_s) and diffuse (f_d) reflector is given as,

$$f_s = \delta(\omega - \omega_r)\cos(\theta_r), \quad (1)$$

$$f_d = \frac{\cos(\theta_r)}{2}, \quad (2)$$

where θ_r is the angle of reflection relative to the reflector's normal, and ω_r is the solid angle in direction of reflection. To simulate glossy reflection, GGX model can be used [14]. The flux received by the x^{th} pixel on a module upon reflection by the y^{th} pixel on the reflector, F_{xy}, is given as,

$$F_{xy} = F_0 \cos(\theta_i - \alpha)\, f_x d\omega \quad (3)$$

where α is the module tilt, f_x is the desired reflection function (f_s for specular, f_g for glossy, and f_d for diffuse), and $d\omega$ is the angular difference between the left and the right edge of the pixel.

Finally, the output for an *x*-*y* pixel pair, J_{xy}, and the total output due to the albedo, $J_{sc,rear}$, is calculated using the following equation,

$$J_{sc,xy} = q \int F_{xy} EQE\,(\lambda,\beta)\cos(\beta)\, d\lambda \quad (4)$$

$$J_{sc,rear} = \sum_y \sum_x J_{sc,xy}/L_m \quad (5)$$

where q is the charge of an electron (1.6×10^{-19} Coulombs), λ is the wavelength, *EQE* is the external quantum efficiency of the module, β is the angle of the incoming flux relative to the normal of the module, and L_m is the width of the module. The EQE used for this work was computationally simulated for a silicon heterojunction bifacial module using SunSolve™, developed by PV Lighthouse. Further details on the architecture and the EQE can be found in [15, 16].

This results in the spectro-angular output contributed by the albedo. The output due to front-side illumination, $J_{sc,front}$, is given as,

$$J_{sc,front} = q \int F_0(\lambda)\cos(\alpha-\theta)\, EQE(\lambda,\beta)\, d\lambda \quad (6)$$

Adding $J_{sc,rear}$ and $J_{sc,front}$ gives the final total output, J_{sc}.

III. Results

We use AM1.5G as the incident flux at θ_i=85˚. The module width is fixed. The reflector width is set to be 10 times the module width and each unit length is divided into 10 pixels. For a horizontally oriented reflector, the algorithm is swept over a range of module tilt (from 30˚ to 90˚ relative to the horizontal axis) and ratio of module height-to-width (from 1 to 3). Although module width was kept constant here, calculating as a function of the height to width ratio will allow comparisons to other module dimensions. Moreover, since module width was fixed, the height-to-width ratio essentially represents module height or separation.

A. $J_{sc,rear}$ with Perfect Specular Reflector

$J_{sc,rear}$ in the presence of a perfect specular reflector with and without self-shading is shown in Fig. 2a and 2b.

1) No self-shading

From Fig. 2a., we observe that the output remains constant despite the changing distance between the module and the albedo surface (i.e., module ratio). This shows that a varying separation has no effect on the module's ability to capture the parallelly reflected irradiance. We also see that the output increases as the tilt increases. This is because the capturing area of the module increases with tilt, and the module accepts the reflected irradiance closer to its own normal.

2) Self-shading included

When we include self-shading (Fig. 2b), overall output decreases. J_{sc} decreases as the separation decreases, since the modules moves nearer to the shadow, and captures less number of parallelly reflected rays. Now, as we go from 30˚ to 90˚, the shadow size increases but is compensated by the fact that the module accepts light closer to its normal, leading to better EQE. All of the above factors result into the optimal configuration being that of higher separation and tilt.

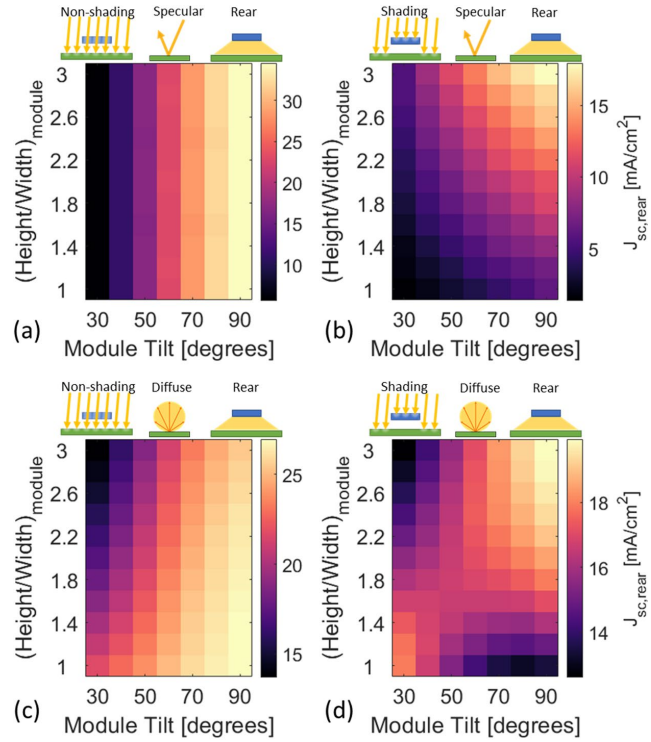

Fig. 2. Module output due to rear-side illumination ($J_{sc,rear}$) as a function of the module height-to width ratio and module when illuminated with AM1.5G at θ_i=85˚ for, a) a perfect specular reflector excluding self-shading, b) a perfect specular reflector including self-shading, c) a perfect diffuse reflector excluding self-shading, d) a perfect diffuse reflector including self-shading.

B. $J_{sc,rear}$ with Perfect Diffuse Reflector

Fig. 2c and Fig. 2d show $J_{sc,rear}$ in the presence of a perfect diffuse reflector with and without self-shading, respectively.

1) No self-shading

In the case of no self-shading (Fig. 2c.), J_{sc} increases as the module moves closer to the albedo surface and as the tilt increases from 30˚ to 90˚. This occurs due to an improve in the capturing ability of the module. Furthermore, at higher separation, and higher tilt the contribution of $\cos(\theta_r)$ is higher. All of this leads to the optimal configuration for non-shading case being that of lower height but higher tilt.

2) Self-shading included

In Fig. 2d., we include the effects of self-shading. Apart from a drop in overall output, we notice a new minima for lower height but higher tilt. This is due to increase in shading as the module goes from 30˚ to 90˚.

C. Comparing Perfect Specular and Perfect Diffuse Reflector

More interesting observations can be made when we compare the output due to the specular and the diffuse reflector. In the case of no self-shading, we see that the specular reflector (Fig. 2a) results in higher J_{sc} as compared to the diffuse reflector (Fig. 2c). When we consider self-shading, the diffuse reflector (Fig. 2d) outperforms the mirror reflector (Fig. 2b) over the

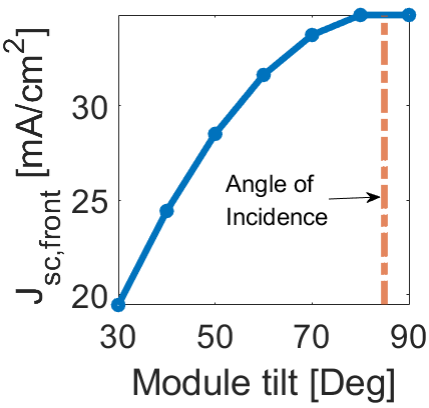

Fig. 3. Module output due to front-side illumination ($J_{sc,front}$) as a function of mdoule tilt when illuminated with AM1.5G at θ_i=85˚.

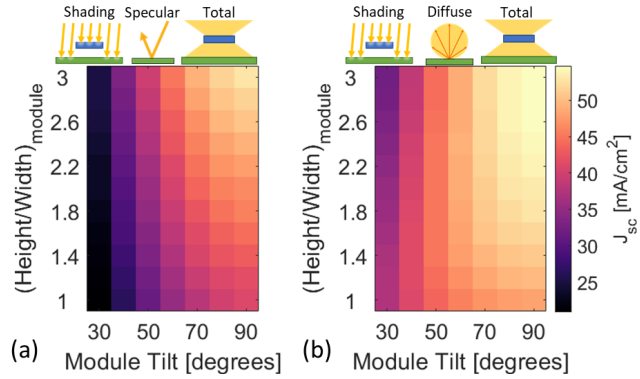

Fig. 4. Total module output (J_{sc}) as a function of the module height-to-width ratio and module tilt when illuminated with AM1.5G at θ_i=85˚, including self-shading, for, a) a perfect specular reflector, b) a perfect diffuse reflector.

entire range of module tilt and module height (or height-to-width ratio). This is because even though the mirror redirects a bigger fraction of incoming irradiance than the diffuser, it does so only in the direction of reflection. If a module is not always strategically positioned over a mirror to minimize shading and maximize light capture (i.e., tracking), it can lead to lower output as compared to a diffuse reflector. Therefore, a diffuse reflector proves to be more robust as it redirects the light with less rigid angular restrictions.

D. Front and rear illumination combined

The final total output, J_{sc}, is calculated by adding $J_{sc,rear}$ (using eq(5)) and $J_{sc,front}$ (using eq(6)). A plot of $J_{sc,front}$ as a function of module tilt is shown in Fig. 3, since a change in module height has no effect on it. Fig. 4a and 4b show J_{sc} for a perfect specular and a perfect diffuse reflector, respectively; both include self-shading. We notice that $J_{sc,front}$ offsets the lower output occurring for higher tilt due to shading. A comparison of Fig. 4a. and 4b. shows us that under non-optimal orientation a specular reflector will perform worse. A diffuse reflector produces higher output for every configuration and is more robust against shading and varying module tilt, as compared to a specular reflector.

IV. Discussion And Conclusion

We presented a computational model that performs reverse-ray tracing on the reflector and can employ diffuse, mirror, and glossy albedo. By implementing the spectral and angular reflectivity, we have developed a more accurate method of quantifying J_{sc} for bifacial modules. Using this model, we investigated the influence of various albedos on silicon heterojunction module with bifaciality of 98.8%. From our study, we conclude that using perfect diffuse and mirror albedo, J_{sc}>54 mA/cm^2 and J_{sc}>52 mA/cm^2 is achievable, respectively. Also, a diffuse reflector is more robust to changes in configuration and, consequently, self-shading.

The study presented here serves as a motivation to expand the reverse ray-tracing algorithm in quantifying the effect of albedo on solar modules. The software permits investigation of general surfaces (*i.e.* diffuse, glossy and specular), and exotic surfaces like metamaterials and luminescent solar concentrators [1, 17]. The presented model enables understanding of albedo-module interplay at a fundamental level. Such an approach can also inspire a more rigorous way of defining surface properties of a reflector for higher PV output. Various existing reflectors (natural and artificial) can be assessed and novel reflectors can designed for higher yield. Furthermore, on combining with open-circuit voltage data and local irradiance or spectro-angular irradiance measurements [16], this methodology will help in determining the best albedo-module pair and configuration for the desired outcome. *E.g.* Highest annual yield, higher yield during sunrise and sunset hours, higher yield during office hours, *etc*.

V. References

[1] L. Einhaus and R. Saive, "Free-Space Concentration of Diffused Light for Photovoltaics," in *47th IEEE PVSC*, 2020.

[2] M. R. Khan, E. Sakr, X. Sun, P. Bermel and M. A. Alam, "Ground sculpting to enhance energy yield of vertical bifacial solar farms," *Applied Energy,* vol. 241, pp. 592-598, 2019.

[3] T. C. R. Russell, R. Saive, A. Augusto, S. G. Bowden and H. A. Atwater, "The Influence of Spectral Albedo on Bifacial Solar Cells: A Theoretical and Experimental Study," *IEEE Journal of Photovoltaics,* vol. 7, no. 6, pp. 1611-1618, 2017.

[4] T. C. R. Russell, R. Saive and H. A. Atwater, "Thermodynamic Efficiency Limit of Bifacial Solar Cells for Various Spectral Albedos," in *44th IEEE Photovoltaic Specialist Conference (PVSC)*, Washington, D.C., USA, 2017.

[5] M. Brennan, A. Abramase, R. Andrews and J. Pearce, "Effects of spectral albedo on solar photovoltaic devices," *Solar Energy Materials & Solar Cells,* vol. 124, pp. 111-116, 2014.

[6] N. Lindsaya, Q. Libois, J. Badosa, A. Migan-Dubois and V. Bourdin, "Errors in PV power modelling due to the lack of spectral and angular details of solar irradiance inputs," *Solar Energy,* vol. 197, pp. 266-278, 2020.

[7] I. Haedrich, M. Ernst, A. Thomson, P. Zheng, X. Zhang, H. Jin and D. Macdonald, "How cell textures impact angular cell-to-module ratios and the annual yield of crystalline solar modules," *Solar Energy Materials and Solar Cells,* vol. 183, pp. 181-192, 2018.

[8] R. Saive, T. C. R. Russell and H. A. Atwater, "Enhancing the Power Output of Bifacial Solar Modules by Applying Effectively Transparent Contacts (ETCs) With Light Trapping," *IEEE Journal of Photovoltaics,* vol. 8, no. 5, pp. 1183-1189, 2018.

[9] N. Tavakoli and Esther Alarcon-Llado, "Combining 1D and 2D waveguiding in an ultrathin GaAs NW/Si tandem solar cell," *Optics Express ,* vol. 27, pp. A909-A923, 2019.

[10] A. Asgharzadeh, M. A. Anoma, A. Hoffman, C. Chaudhari, S. Bapat, R. Perkins, D. Cohen, G. M. Kimball, D. Riley and F. Toor, "A Benchmark

and Validation of Bifacial PV Irradiance Models," in *IEEE 46th Photovoltaic Specialists Conference (PVSC)*, Chicago, IL, USA, 2019.

[11] C. E. Valdivia, C. T. Li, A. Russell, J. E. Haysom, R. Li, D. Lekx, M. M. Sepeher, D. Henes, K. Hinzer and H. P. Schriemer, "Bifacial Photovoltaic Module Energy Yield Calculation and Analysis," in *IEEE 44th Photovoltaic Specialist Conference (PVSC)*, Washington, DC, 2017.

[12] T. O. Fartaria and Manuel Collares Pereira, "Simulation and computation of shadow losses of direct normal, diffuse solar radiation and albedo in a photovoltaic field with multiple 2-axis trackers using ray tracing methods," *Solar Energy,* vol. 91, pp. 93-101, 2013.

[13] M. R. Vogt, T. Gewohn, C. Schinke and R. Brendel, "Impact of using spectrally resolved ground albedo data for performance simulations of bifacial modules," in *EUPVSEC 2018*, 2018.

[14] B. Walter, S. Marschner, H. Li and K. Torrance, "Microfacet Models for Refraction through Rough Surfaces," in *Proceedings of the Eurographics Symposium on Rendering Techniques*, Grenoble, France, 2007.

[15] R. Saive and T. C. R. R. a. H. A. Atwater, "Light Trapping in Bifacial Solar Modules Using Effectively Transparent Contacts (ETCs)," in *IEEE 7th World Conference on Photovoltaic Energy Conversion (WCPEC)*, Waikoloa Village, HI, USA, 2018.

[16] S. Pal, A. Reinders and R. Saive, "Simulation of Bifacial and Monofacial Silicon Solar Cell Short-Circuit Current Density Under Measured Spectro-Angular Solar Irradiance," *IEEE Journal of Photovoltaics,* vol. 10, no. 6, pp. 1803-1815, 2020.

[17] G. Heres, L. Einhaus and R. Saive, "Analytical Model for the Performance of a Free-Space Luminescent Solar Concentrator," in *IEEE Photovoltaic Specialists Conference (PVSC)*, online, 2021.